Bottom temperature and salinity distribution and its variability around Iceland

Kerstin Jochumsen [a,*], Sarah M. Schnurr [b], Detlef Quadfasel [a]

[a] Institut für Meereskunde, Universität Hamburg, Bundesstrasse 53, 20146 Hamburg, Germany
[b] Senckenberg am Meer, German Center for Marine Biodiversity Research (DZMB), c/o Biocentrum Grindel, Martin-Luther-King Platz 3, 20146 Hamburg, Germany

ABSTRACT

The barrier formed by the Greenland–Scotland-Ridge (GSR) shapes the oceanic conditions in the region around Iceland. Deep water cannot be exchanged across the ridge, and only limited water mass exchange in intermediate layers is possible through deep channels, where the flow is directed southwestward (the Nordic Overflows). As a result, the near-bottom water masses in the deep basins of the northern North Atlantic and the Nordic Seas hold major temperature differences.

Here, we use near-bottom measurements of about 88,000 CTD (conductivity–temperature–depth) and bottle profiles, collected in the period 1900–2008, to investigate the distribution of near-bottom properties. Data are gridded into regular boxes of about 11 km size and interpolated following isobaths. We derive average spatial temperature and salinity distributions in the region around Iceland, showing the influence of the GSR on the near-bottom hydrography. The spatial distribution of standard deviation is used to identify local variability, which is enhanced near water mass fronts.

Finally, property changes within the period 1975–2008 are presented using time series analysis techniques for a collection of grid boxes with sufficient data resolution. Seasonal variability, as well as long term trends are discussed for different bottom depth classes, representing varying water masses. The seasonal cycle is most pronounced in temperature and decreases with depth (mean amplitudes of 2.2 °C in the near surface layers vs. 0.2 °C at depths >500 m), while linear trends are evident in both temperature and salinity (maxima in shallow waters of +0.33 °C/decade for temperature and +0.03/decade for salinity).

© 2016 Published by Elsevier Ltd.

1. Introduction

The near-bottom water masses in the deep basins of the northern North Atlantic and the Nordic Seas hold major temperature differences due to the barrier formed by the Greenland–Scotland-Ridge (GSR). A direct exchange of deep water across the ridge is not possible, and only limited water mass exchange in intermediate layers takes place through several channels, where the flow is southward (the Nordic Overflows; Hansen and Østerhus, 2000). The influence of this topographic barrier can be connected to species distributional patterns and to the species composition of specific benthic organisms (e.g. Weisshappel, 2001; Dijkstra et al., 2009; Brix and Svavarsson, 2010), as the exchange between benthic organisms for bottom depths exceeding about 500 m is also restricted.

Surface-intensified, northward flow across most of the GSR brings warm and saline waters into the Nordic Seas, which are carried within the three current branches of the North Atlantic Current: The Iceland branch, the Faroe branch and the Shetland branch (Østerhus et al., 2005). At the western GSR (along the east Greenlandic coast) cold and fresh water is transported southwestward within the East Greenland Current. Interchanges of some benthic species are thus possible along the shelf regions within these currents, which also provide a possible pathway for the spreading of invading species. As recent studies already found evidence for increasing temperatures in Arctic and Subarctic waters as well as in the shallower regions around Iceland within the last 10 years (Astthorsson et al., 2007; Larsen et al., 2012; Yashayaev and Seidov, 2015), it seems likely that climate alterations will also have an effect on organisms living within the affected region.

Several abiotic factors such as sediment type (Stransky and Svavarsson, 2010), temperature and salinity (Mayer and Piepenburg, 1996), as well as bathymetry (Schnurr et al., 2014; Dauvin et al., 2012), are known to shape and influence community composition and species distributions in Arctic and Subarctic regions.
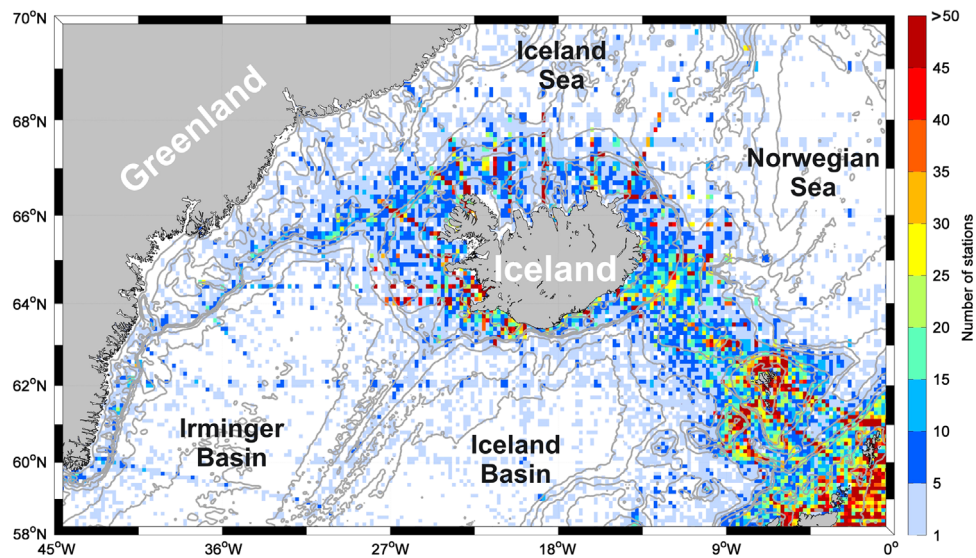

Fig. 1. Gridded data distribution of near-bottom temperature measurements in the area of investigation. The overall maximum number of measurements for a few grid cells is exceeding 300 and is thus out of scale, which was adjusted to the range of the most common numbers of measurements in the cells. The bottom depth is taken from ETOPO2 bathymetry and contours illustrate the [5000 4000 3000 2000 1500 1000 500 300 100] m depth levels.

Information on these spatially changing environmental variables in combination with species distribution data can be used for species distribution modeling (SDM), which is a tool for a better understanding of species distributions within the marine environment (Elith and Graham, 2009). These models can provide an estimate of the response of the marine ecosystem and species distributions to climate change.

In this work we use near-bottom temperature and salinity measurements to obtain spatial property distributions north and south of the GSR (Fig. 1), which have already been used to create realistic SDMs (Meißner et al., 2014). Local variability is discussed according to the standard deviations within the region, which reflects the uncertainty of the distributions, as well as highlights ocean variability (e.g. oceanic fronts or migrating currents). Additionally, we analyse the hydrographic changes on seasonal and longer time scales within the last 30 years.

2. Data selection and quality control

The hydrographic data used in this study were extracted from the NISE data base (Norwegian Iceland Seas Experiment, http://monarch-a.nersc.no/node/45 and Nilsen et al., 2008), which is composed of 509,625 hydrographic stations. The NISE project is a joint venture of research institutions in Iceland (MRI, Marine Research Institute), the Faroe Islands (HAVSTOVAN, Faroe Marine Research Institute), and Norway (IMR, Institute of Marine Research; GFI, Geophysical Institute). NISE contains hydrographic data records of over 100 years and is based on the ICES data set (International Council for the Exploration of the Sea, www.ices.dk), which is the most comprehensive in the region of interest and has undergone established quality control. The ICES data have been complemented with data from the contributing research institutions, as well as other online sources such as WOCE (Word Ocean Circulation Experiment, www.woce.org and Argo (www.usgodae.org). An additional general outlier removal has been performed in the creation of the NISE database (see Nilsen et al., 2008 for more details). Compared with more recent climatological collections such as the NOAA Atlas of the Nordic Seas (Korablev et al., 2014) NISE has a similar data resolution in the early years. Nevertheless, the NOAA Atlas covers a larger area and will be maintained in the future; therefore it is recommended for follow-up studies. The geographical region that encompasses the NISE project spans from the Subpolar North Atlantic Ocean (east of 55°W and north of 50°N) to the GSR and the Iceland and Norwegian Seas. The original NISE data set ended in 2006, but the data base is updated infrequently by J.E.Ø. Nilsen, who provided the NISE data, including the years 2007 and 2008 for this study. In total, 103,378 stations were found within the area of investigation (70°N–58°N, 45°W–0°W).

Historical measurements of temperature and salinity were achieved by collecting water samples in Nansen and Niskin bottles, and since the 1980s electronically by using CTD (Conductivity Temperature Depth) profilers. The data coverage is increasing from sparse in the first half on the last century to more than 1500 measurements per year in recent years (see Fig. A1 in the Appendix). The majority of the profiles was collected between April and September, while sampling effort was least in wintertime. Data coverage is best in the shelf regions around Iceland and the Faroe Islands, as well as along the GSR, whereas only a few stations are available from the deep Irminger and Iceland Basins and the deeper areas of the Iceland and Norwegian Seas.

Since the focus of this study is on the bottom distribution of temperature and salinity, only the deepest measurements of each profile were considered. In order to guarantee that these really provide near-bottom information, the data set was quality-controlled regarding the depth information. A probable bottom depth was allocated to all stations with missing bottom depth information, which was extracted from ETOPO2 (provided by NOAA, see Acknowledgments). The ETOPO2 data base for the region south of 64°N consists of the Smith and Sandwell bathymetry (Smith and Sandwell, 1997) and north of 64°N of the International Bathymetric Chart of the Arctic Ocean (Jakobsson et al., 2000). Closest ETOPO2 latitude and longitude positions were used to assign bottom depths to stations (which lacked bottom depth in the data set) in order to allocate a bottom depth to the given station. Additionally all bottom depths provided in the NISE data set were compared with ETOPO2. All stations with a difference in bottom depth between NISE and ETOPO2 of more than 200 m were excluded from further analysis, as for these stations the real bottom depth is either unknown or the profile did not reach the near-bottom layer. Only stations with a maximum distance of up to 80 m between the last measurement within the profile and the bottom were used in this study.

The choice of the 80 m threshold is a compromise between maintaining as many data points as possible and reducing the noise due to too shallow measurements. The change of temperature with depth is in general largest in the upper ocean thermocline, while the impact of a depth change in the deep ocean is small, except for the overflow regions. But with a typical total overflow plume thickness of 150–300 m (e.g. Macrander et al., 2007), which contains a homogenous bottom layer, our threshold of 80 m is reasonable. Gradients are elevated at water mass boundaries, but stay well below thermocline values. Errors associated with too shallow data are therefore most likely to impact the shallow shelf regions. However, as the data coverage is best here, outliers will not reduce the validity of our results. The errors in the deep layers are of smaller magnitude, also due to the mixing of the near-bottom layer by bottom friction. All temperatures given are in situ temperatures, as for some older data no corresponding pressure measurements were available (only depth information). The difference between in situ temperatures and potential temperatures is below 0.05 °C for water depths shallower than 500 m, which is much smaller than the signals considered. At depth levels exceeding 2000 m the difference between potential temperature and in situ temperature is still <0.2 °C. Salinity is given as practical salinity on the PSS-78 scale throughout the paper. After quality control 88,046 stations with bottom temperature measurements were available within the investigated area. The amount of stations with bottom salinity data was slightly lower (79,856 stations in total).

3. Results

3.1. Analysis of near-bottom temperature and salinity data

The research area was gridded into boxes, with regular steps in longitudinal direction of 0.2° and 0.1° in latitudinal direction (approx. 11 km resolution, cf. Fig. 1). Mean values of temperature and salinity for the period 1900–2008 were calculated for each grid cell (Figs. A2 and A3 in the Appendix), as well as their standard deviation. Subsequently they were interpolated along topography (following f/H contours as described in Davis, 1998), as ocean currents tend to follow isobaths in a low stratification environment. This approach deviates from standard climatologies,
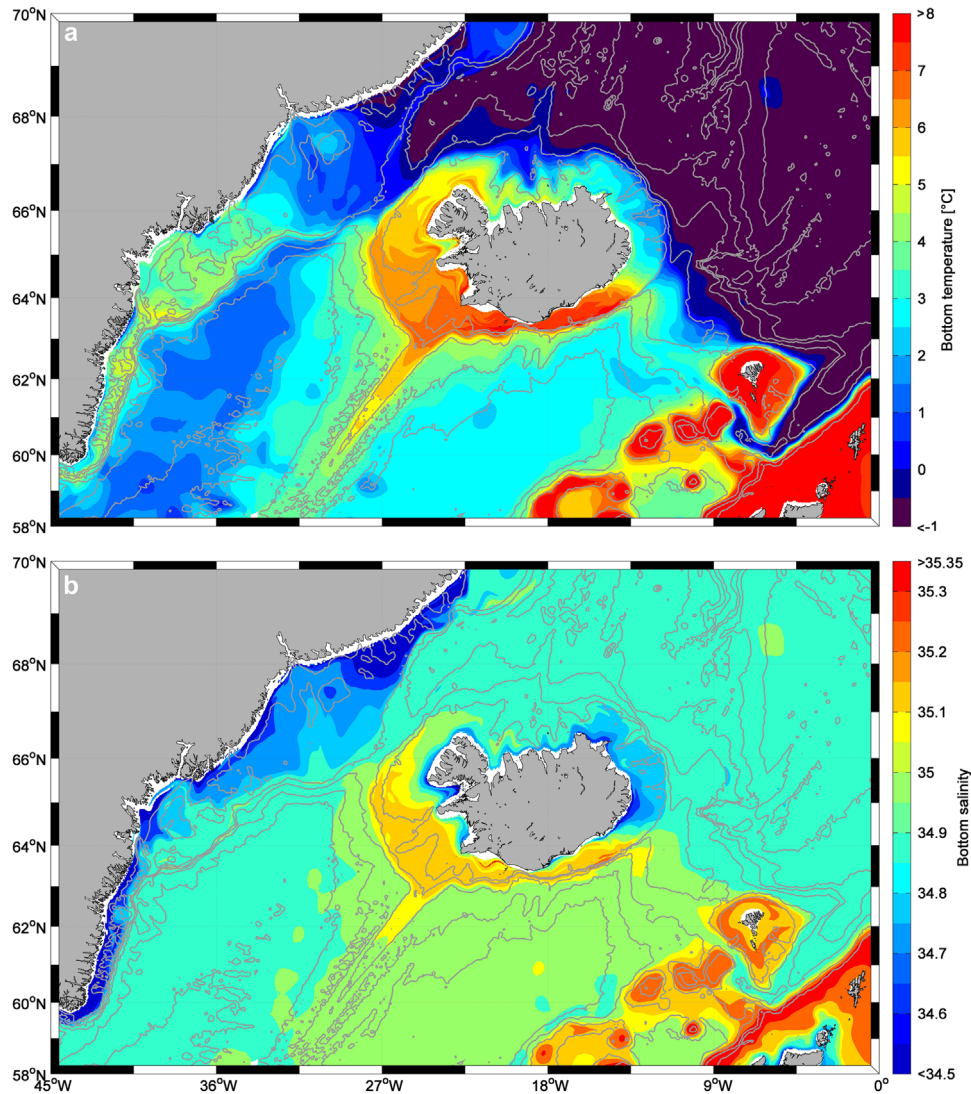

Fig. 2. Interpolated gridded mean bottom properties using the average of the period 1900–2008. (a) Temperature; (b) salinity. Colorscales have been adjusted to represent the range of most common values; out-of-scale values are included in the red and blue colors of the scale endings. An interpolation scheme following isobaths (f/H contours, see Davis, 1998 for details) was applied. The bottom depth contours illustrate the [3000 2000 1500 1000 500 250] m depth levels. (For interpretation of the references to color in this figure caption, the reader is referred to the web version of this paper.)

which commonly use other interpolation schemes such as Optimum Interpolation or Data Interpolating Variational Analysis and are only available at fixed depth levels (such as the NOAA Atlas of the Nordic Seas).

The interpolated near-bottom temperature and salinity values for the whole research area are shown in Fig. 2. A tendency of decreasing temperature values from south to north can be noticed, as well as higher temperatures in shallow areas. The GSR clearly separates the deep basins: near-bottom temperatures in the Iceland and Norwegian Sea deeper than 500 m range between −1 °C and −0.5 °C, while the Iceland and the Irminger Basins are characterized by water temperatures of about 1–3 °C. The salinities of all four basins, as well as in most of the Denmark Strait region, cover a range between 34.8 and 35.0. The range of the hydrographic properties is largest at shallow depths and confined to a distinct T/S space at depths exceeding 500 m, which is illustrated in the temperature–salinity diagram in Fig. A4, as well as in the corresponding profiles shown in Fig. A5.

The region between Greenland and Iceland is influenced by the shallow East Greenland Current and the Denmark Strait overflow.

Both currents flow southwestward along the Greenland coast and shelfbreak. The overflow is seen as a narrow band of low bottom temperatures connecting the basins north and south of Denmark Strait. Bottom temperatures on the Greenlandic shelf range from −1 °C to 2 °C north of Denmark Strait and are 2 °C to 5 °C between Denmark Strait and Cape Farewell. Here, East Greenland Current Waters mix with Atlantic Waters in the Irminger Current, which leads to warmer waters south of Denmark Strait on the Greenlandic shelf. Salinity close to the Greenlandic shore is low (33.6–33.7, due to local ice and glacial melt) compared to all other regions of the research area, but increases to 34.6–34.8 below depths of about 400 m further offshore.

Highest temperatures are found in the southeastern region of the study area, as well as around Iceland. The north-western part of the Icelandic shelf features temperatures of up to 7 °C, where the North Icelandic Irminger Current is present, decreasing to about 2.5 °C in the northeastern part of the Icelandic shelf. Salinities in the north-western part of the Icelandic shelf are between 35.1 and 35.2, and between 34.7 and 34.8 on the northern part of the Icelandic shelf. Lowest salinities around Iceland are found
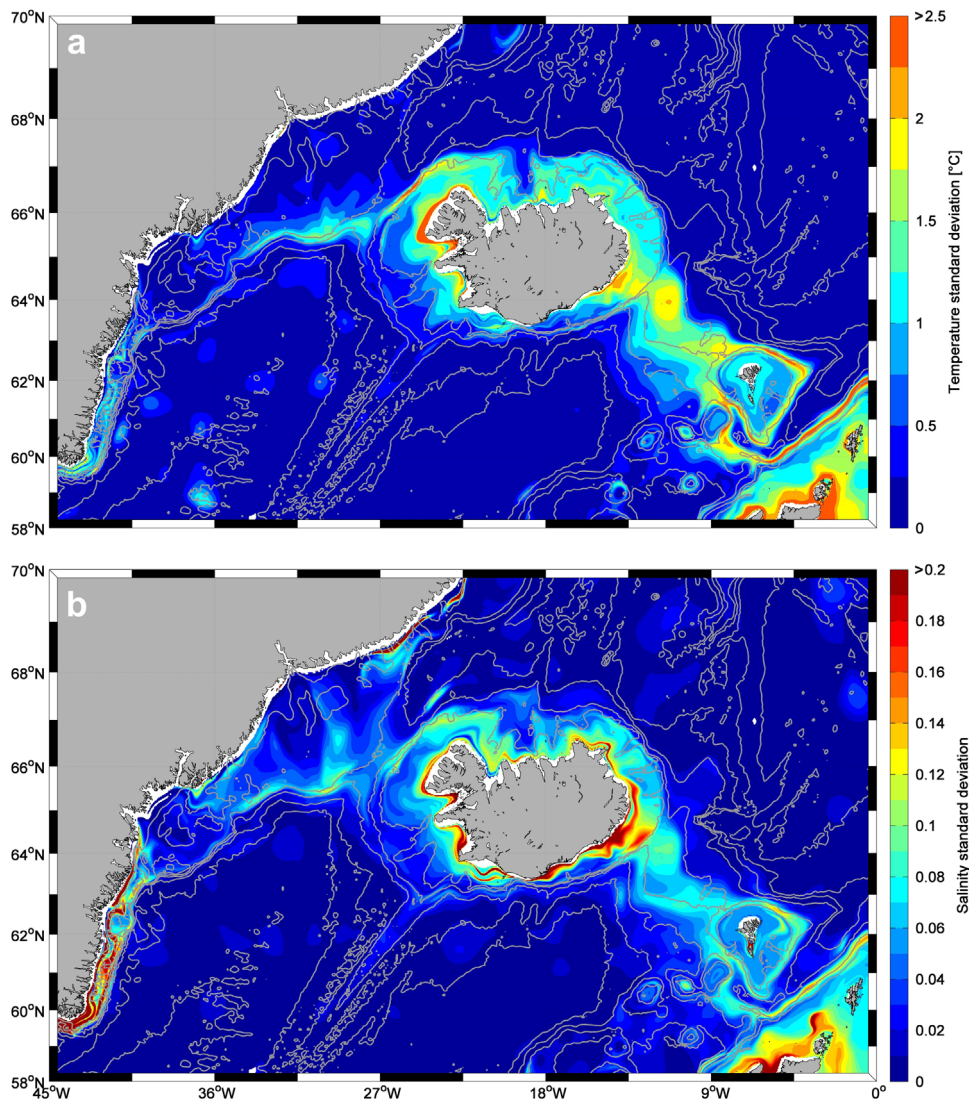

Fig. 3. Interpolated gridded standard deviation of bottom properties of the period 1900–2008. (a) Temperature; (b) salinity. Colorscales have been adjusted to represent the range of most common values; out-of-scale values are included in the red color at the end of the scale. An interpolation scheme following isobaths (f/H contours, see Davis, 1998 for details) was applied. The bottom depth contours illustrate the [3000 2000 1500 1000 500 250] m depth levels. (For interpretation of the references to color in this figure caption, the reader is referred to the web version of this paper.)
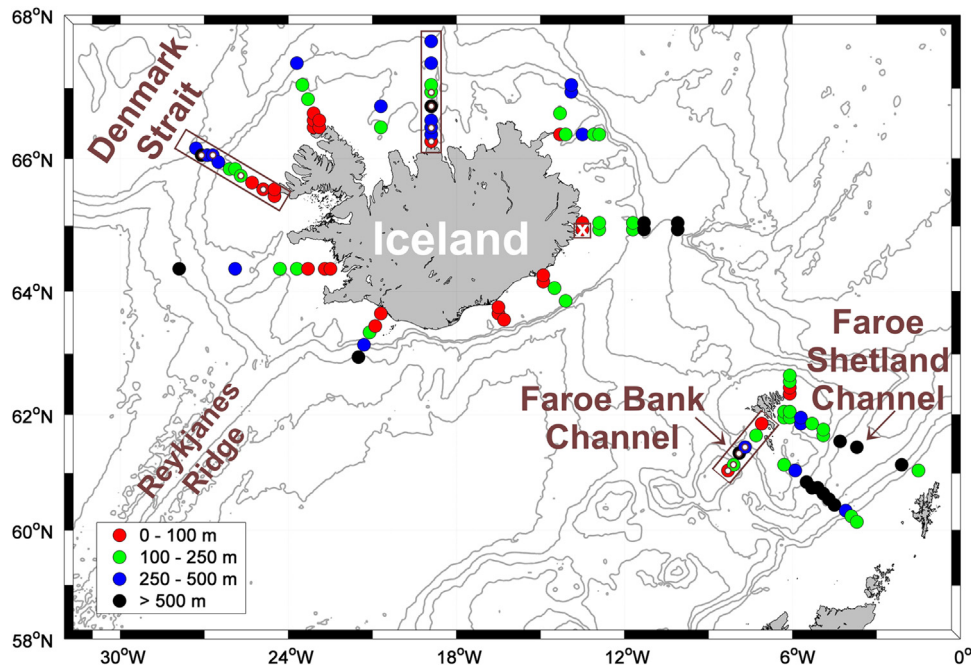
Fig. 4. Grid cells with more than 100 near-bottom data points in the period 1975–2008, which were selected for further analysis. The cells were ordered into classes according to the average depth in each cell. Red: 0–100 m; green: 100–250 m; blue: 250–500 m; black: deeper than 500 m. Pointed out is a cell east of Iceland (brown box and white x), which is used as an exemplary cell for explaining the analysis of the seasonal cycle and trend applied to all presented cells, as illustrated in Fig. 5. Exemplary cells for each depth class were taken from Denmark Strait, a section north of Iceland and the Faroe Bank Channel (brown boxes, white dots in the selected cells) for a comparison of seasonality as shown in Fig. 6. The bottom depth contours illustrate the [3000 2000 1500 1000 500 250] m depth levels. (For interpretation of the references to color in this figure caption, the reader is referred to the web version of this paper.)

close to the eastern and north-eastern shore, with values of approx. 34.4, which are caused by river runoff and low-salinity water transports via the East Icelandic Current, originating from the East Greenland Current.

The shallow GSR ridge east of Iceland and close to Scotland exhibits the highest temperatures, which are associated with the branches of the North Atlantic Current crossing the GSR in this region. The shallowest region of the GSR between Iceland and the Faroe Islands features bottom temperatures of up to 4.5 °C and mean salinities of 35–35.1. The water temperatures on the coastal region around the Faroe Islands (up to 11 °C) show the highest temperatures within the whole area considered here. Salinity values in this part are between 35.1 and 35.3. In addition, cold overflowing waters (− 1 °C to − 0.5 °C) are recognized in the Faroe Bank Channel between the Faroe Bank and the Faroe Plateau. Entrainment into the overflow is indicated by the subsequent warming of the bottom temperatures along the channel, when following the overflow pathway from the Faroe Shetland Channel into the North Atlantic. Salinity in the Faroe Bank Channel is the same as in the Nordic Basins (34.8–34.9). Similar to the temperature distribution a slight increase of salinity (to values from 35 to 35.1) is recognized when the water enters the North Atlantic.

3.2. Distribution of bottom temperature and salinity variability

The variability of bottom properties is reflected in their respective standard deviation, as presented in Fig. 3. For temperature and salinity the distributions of enhanced variability are similar. Standard deviations are highest around Iceland, on the Scottish and Faroe Island shelfs, and along the GSR. These shallow regions are more directly influenced by the variability in air–sea fluxes. Here, standard deviations are up to 2.5 °C in temperature and 0.2 in salinity. Standard deviations in the basins of the deep ocean regions are rather low (below 0.5 °C in temperature and 0.05 in salinity). Exceptionally high variability is found in the

salinity south of Greenland (up to 0.6) and around Iceland (about 0.3), which is caused by seasonally varying river run off, ice melt and intra- and interannual variability of these processes. Additionally, elevated standard deviations are found at steep slopes, such as the sides of the Faroe Shetland Channel, Denmark Strait and the shelf breaks. The gridding method used in this study cannot resolve steep slopes and data with large bottom depth differences are averaged in these boxes, which induces artificially high variance. Furthermore, downstream of the sills of the GSR the overflows descend into the deep basins and are modified by turbulent entrainment, which induces strong variability (e.g. Fer et al., 2010; Voet and Quadfasel, 2010). The GSR between Iceland and the Faroe Islands exhibits high variability of the bottom properties due to the intermittent nature of the overflow crossing this part of the ridge (e.g. Østerhus et al., 2008). The overflow branch crossing the Wyville Thomson Ridge is also recognizable in the distribution of standard deviation due to its high variability (Sherwin et al., 2008).

The influence of single outliers in the data, which are probably present even in the quality-controlled data set, is most pronounced on this part of our analysis. However, due to the high data coverage along the GSR (see Fig. 1) the standard deviations are robust in this region. The standard deviation obtained from the sparse data in the deep basins is in contrast more sensitive regarding single bad data points, which will increase the standard deviations. The patches of elevated variability in the basins (e.g. at 62°N/30°W in the Irminger Basin) are therefore considered to be artefacts (order of 0.5 °C in temperature and 0.02 in salinity).

3.3. Time series of bottom temperature and salinity

In the following, only grid boxes containing more than 100 near-bottom data points in the period 1975–2008 were considered, as sufficient data coverage is needed to carry out time series analysis. Huge data gaps occur in most time series in the

Table 1
Summary of the temperature time series analysis. Depth class: depth class of grid cell as shown in Fig. 4; boxes: amount of grid boxes for the given depth class; season: averaged amplitude of the seasonal variability for temperature in the given depth class (in °C); expl. var.: percentage of explained variance from seasonal variability; trend: averaged decadal temperature trend in the given depth class (in °C/10 years); expl. var.: percentage of explained variance from the trend in the de-seasoned temperature time series; residual: standard deviation of the de-seasoned and de-trended residual (in °C).

Depth class (m)	Boxes	Season	Expl. var. (%)	Trend	Expl. var. (%)	Residual
0–100	27	2.2	72	0.33	16	0.8
100–250	36	1.1	53	0.31	20	0.7
250–500	21	0.4	12	0.13	10	0.7
>500	18	0.2	7	0.05	7	0.4

Table 2
Summary of the salinity time series analysis. Depth class: depth class of grid cell as shown in Fig. 4; boxes: amount of grid boxes for the given depth class; season: averaged amplitude of the seasonal variability for salinity in the given depth class; expl. var.: percentage of explained variance from the seasonal variability; trend: averaged decadal salinity trend in the given depth class (in 1/10 years); expl. var.: percentage of explained variance from the trend in the de-seasoned salinity time series; residual: standard deviation of the de-seasoned and de-trended residual. Grey numbers denote correlation results with more than half of the boxes below the 95% confidence limit.

Depth class (m)	Boxes	Season	Expl. var. (%)	Trend	Expl. var. (%)	Residual
0–100	26	0.06	8	0.03	10	0.12
100–250	34	0.03	12	0.03	18	0.06
250–500	18	0.02	3	0.01	9	0.05
>500	18	0.01	2	<0.01	14	0.02

period from 1900 to 1975, therefore the analysis starts in 1975, from whereon the time series are continuous. The 102 selected temperature grid boxes (96 for salinity) were sorted into depth classes according to the average bottom depth within each box (Fig. 4): 0–100 m (depth class 1), 100–250 m (depth class 2), 250–500 m (depth class 3) and >500 m (depth class 4). The data resolve the shallow shelf areas around Iceland and the Faroe Islands, but the deep basins lack a sufficient amount of data. Nevertheless, at the sills of the GSR (namely: the Denmark Strait, the Faroe Bank Channel and the Faroe Shetland Channel) enough data for the time series analysis are available. A summary of the analysis is given in Tables 1 and 2.

3.3.1. Seasonal variability

For each of the selected cells the average seasonal cycle was determined by fitting a harmonic oscillation to the time series in a least-squares sense. Significance was tested by correlating the derived seasonality with the original time series. One example for temperature in depth class 1 (0–100 m) is shown in Fig. 5a, illustrating the harmonic fit. The temperature time series exhibits a significant seasonal cycle representing the mean seasonality of this depth class in temperature (amplitude 2.2 °C, Table 1), explaining 77% of the variance within this specific time series. Average seasonal amplitudes and the correspondingly explained variance are given for the four depth classes in columns 3 and 4 in Table 1 for the temperature measurements and in Table 2 for the salinity measurements. The seasonal amplitude rapidly decreases with depth, as well as the variance explained by the seasonality. Seasonality in salinity is mostly not significant within the depth classes 3 and 4. In depth class 2 the explained variance by the seasonal cycle is higher than for depth class 1 in salinity, which
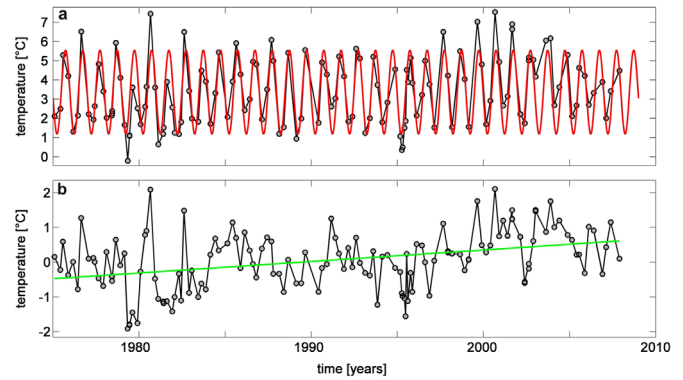

Fig. 5. (a) Time series of temperature measurements (grey) and seasonal cycle (red) of an exemplary grid cell in the depth range 0–100 m east of Iceland (see Fig. 4). The lower panel (b) shows the de-seasoned temperature anomalies (grey) and the derived temperature trend (green) for this exemplary box. (For interpretation of the references to color in this figure caption, the reader is referred to the web version of this paper.)
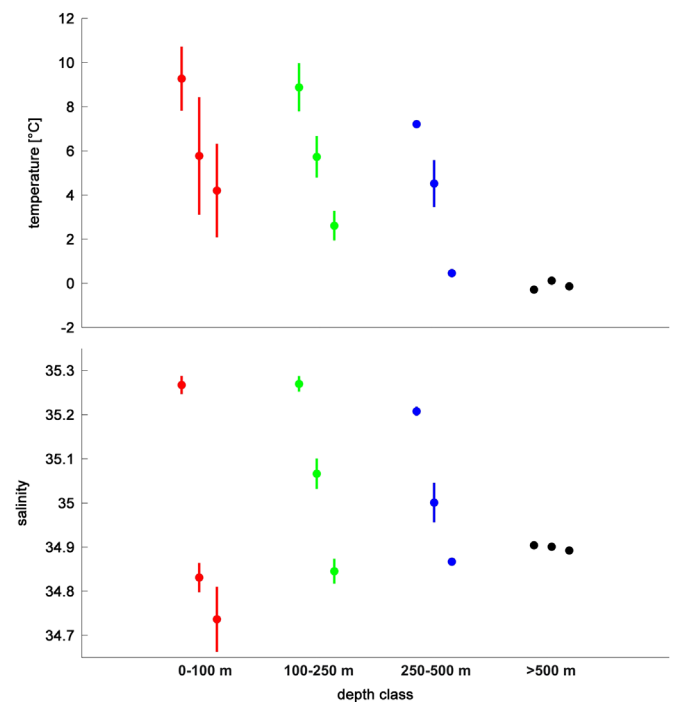

Fig. 6. Average temperature (upper panel) and salinity (lower panel) values with seasonal variations (vertical bars) for exemplary boxes of each depth class at three sections (highlighted in Fig. 4). The left point of each depth class is from the section in the Faroe Bank Channel, the middle point from Denmark Strait and the right point from north of Iceland.

might be caused from less intra-seasonal influences on deeper levels like strong rainfall events during storms.

A comparison of seasonality for different depth classes and locations is presented in Fig. 6. Examples of all depth classes from three sections located (1) in the Faroe Bank Channel, (2) in Denmark Strait and (3) north of Iceland are depicted regarding the mean value and its seasonal variation. Average temperatures and salinities are highest in the Faroe Bank Channel and lowest north of Iceland. Seasonality in general decreases with depth and is often not significantly different from zero at depth >250 m. An exception is depth class 3 (250–500 m) in Denmark Strait, where the temperature and the salinity still exhibit seasonal variations. Additionally, for the deep waters north of Iceland and in the Faroe
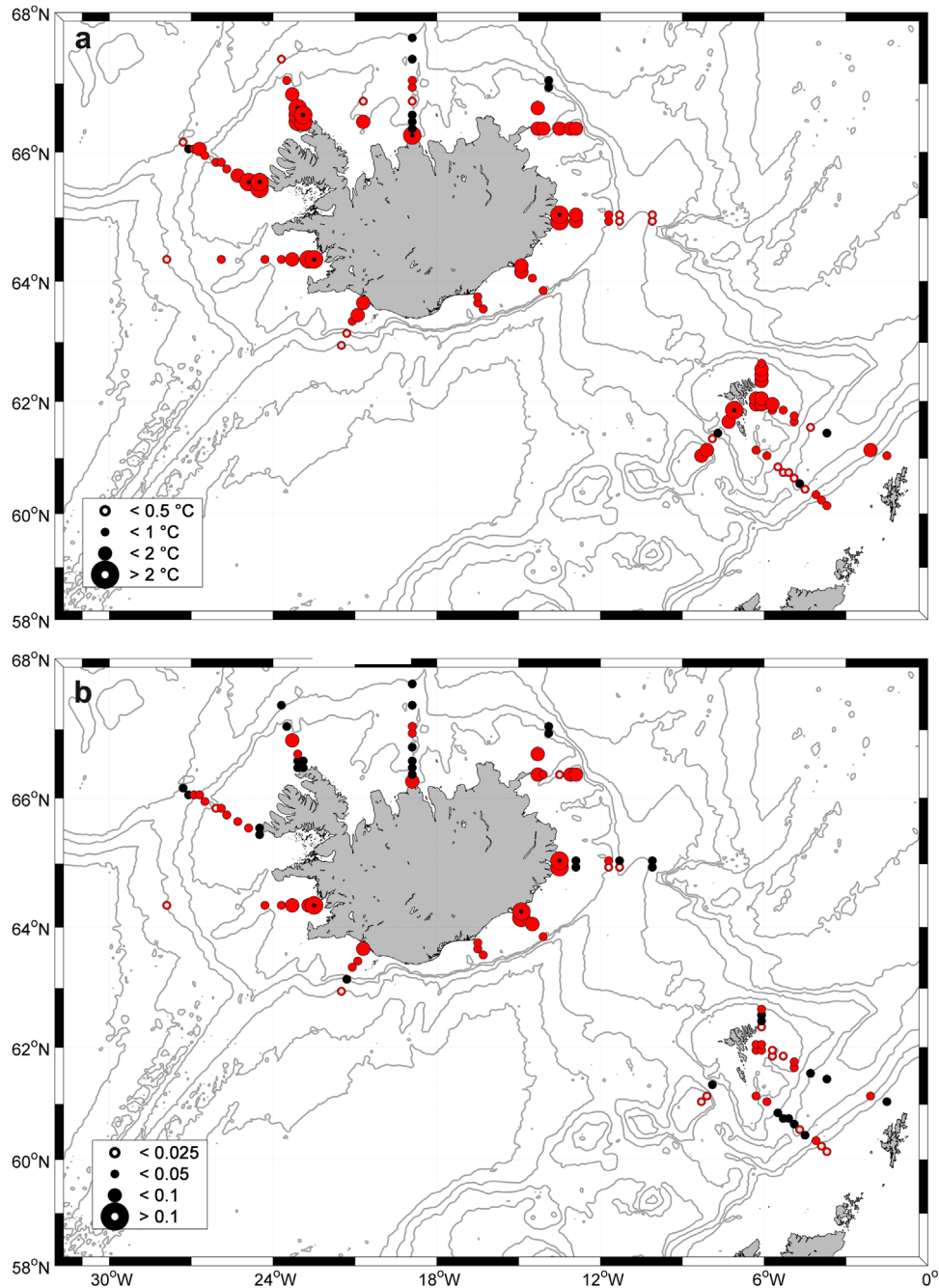
Fig. 7. Amplitude of the seasonal cycle for temperature (a) and salinity (b) for the selected grid boxes of Fig. 4. Black colors denote boxes with no significant seasonality, red colors mark significant harmonic oscillations. The size of the circle gives the amplitude (see figure legend, smallest and largest amplitudes have a dot in the middle of the marker). The bottom depth contours illustrate the [3000 2000 1500 1000 500 250] m depth levels. (For interpretation of the references to color in this figure caption, the reader is referred to the web version of this paper.)

Bank Channel (depth class 4, >500 m) a significant seasonal amplitude in temperature of about 0.1 °C was found (too small to be seen in Fig. 6). The exemplary boxes shown in Figs. 5 and 6 illustrate the importance of the seasonal variability in temperature at shallow depth levels, which is the dominating signal in all these time series. In contrast, variability in salinity is less controlled by the seasonal cycle, but experiences variability on other timescales.

The spatial distribution of the seasonal amplitude is depicted in Fig. 7. Seasonality is most pronounced in the shelf areas, where not only the water depth is very shallow, but also seasonal river run off may play a role. Especially for salinity the seasonal amplitude is elevated near the southern coast of Iceland. Deep grid boxes often

do not exhibit any significant seasonality.

3.3.2. Temperature and salinity trends

The time series were tested for long term trends using temperature and salinity anomalies, which were obtained by subtracting the seasonal signal from the measurements. Significance was derived from Student's *t*-test, using the 95% significance limit. An example of the de-seasoned anomalies with the respective trend line is given in Fig. 5b. The shown trend is significant (+0.38 °C/10 years) and explains 15% of the variance evident in the anomalies. Significant linear trends were found for the majority of the grid boxes, which explain at maximum 20% of the
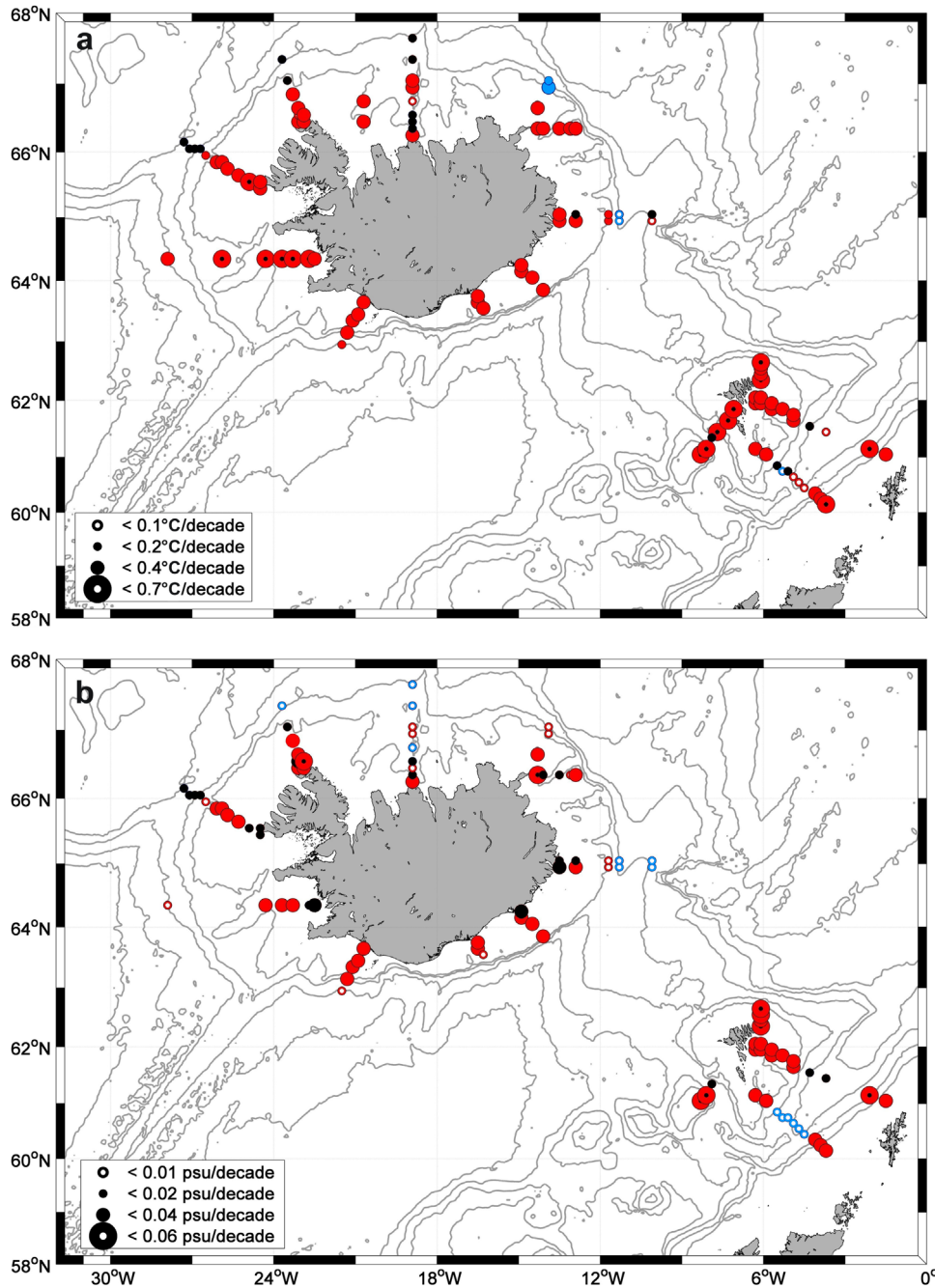
Fig. 8. Temperature (a) and salinity (b) trends in relation to a 10 year period for the selected grid boxes of Fig. 4. Blue colors denote negative trends and red colors mark positive trends. Black colors denote boxes with no significant trend (95% significance limit). The size of the circle gives the magnitude of the trend (see figure legend, smallest and largest trends have a dot in the middle of the marker). The bottom depth contours illustrate the [3000 2000 1500 1000 500 250] m depth levels. (For interpretation of the references to color in this figure caption, the reader is referred to the web version of this paper.)

variance present in the anomalies (columns 5 and 6 in Tables 1 and 2, respectively). The majority of the trends is positive. However, the magnitudes of the trends are rather small compared to the total variability; hence they might go unnoticed in shorter time series. The trend analysis points again at decreasing signal strength with depth: the magnitudes of the trends are highest at shallow depth levels. However, the relative importance of the trend for the variability of the time series (explained variance) remains similar for all depth classes, at least in salinity.

A summary of the derived trends is given in Fig. 8, where the magnitude and position of the trends is illustrated. Strong positive trends are evident on the shallow shelf regions near Iceland and

the Faroe Islands, while trends in the deep channels like Denmark Strait and the Faroe Bank and Shetland Channels are around zero (below 0.1 °C/10 years and 0.01/10 years; both positive and negative and often not significant). The most prominent negative trend is found on the northeastern Icelandic slope; a region where supposedly the North Icelandic Jet originates (Våge et al., 2013), a current contributing to the Denmark Strait Overflow. Small negative trends in salinity are found at deep locations, e.g. in the Faroe-Shetland Channel.

3.3.3. Residual variability

A residual variability has been calculated by subtracting both,

the seasonal cycle and the long term trend, from the data. The variability still present in this residual is expressed as the standard deviation of the de-seasoned, de-trended temperature and salinity anomaly as given in the last columns of Tables 1 and 2. This residual variability is for most depth classes in the same order of magnitude or even above the seasonal cycle. For the exemplary grid box in Fig. 5 the standard deviation of the residual variability is 0.8 °C in temperature. No significant correlation with large scale atmospheric forcing (NAO; Hurrell, 1995) or the Atlantic Multi-decadal Oscillation (AMO; Enfield et al., 2001) has been found; these residual variations are therefore likely effects of local forcing, e.g. storms or exceptional ice melt. Additionally, the uncertainty of the data set due to errors in the depth calculation (see data selection and quality control) and the gridding method contributes to the residual, as well as aliasing effects.

4. Summary and discussion

About 88,000 hydrographic near-bottom measurements are used in this study to obtain the average distribution of temperature and salinity around Iceland, at the Greenland-Scotland-Ridge and in the deep basins north and south of the ridge. The quality-controlled data have been gridded into regular boxes, in which the hydrographic properties are averaged. The mean properties as well as the standard deviation are then interpolated using a depth-following algorithm, as currents in the region tend to follow isobaths. In the resulting maps the influence of the ridge system is clearly visible; the cold waters of the Nordic Seas are confined to the area north of the GSR. Additionally, the impact of air–sea–land exchanges in shallower water depths is indicated by the high variability within shelf regions. The dense overflow waters are present in the mean distributions in the deep channels of the GSR, as well as their dilution by entrainment of ambient waters, which is a highly variable process and also reflected by the enhanced standard deviation along their pathways on the Atlantic side of the ridge. The noted variability can drive variability in species distribution patterns, as specific species occupy habitats of defined conditions only. One example is the drift of cod larvae on the North Icelandic Shelf, which is known to depend on the strength of the northeastward Atlantic Water flow on the shelf (Jónsson and Valdimarsson, 2005).

The near bottom temperature and salinity maps created within this study are an important component for the creation of SDMs of benthic species within Icelandic waters (e.g. Meißner et al., 2014) and will help future studies on species distribution patterns. Ecological consequences such as the alteration of species distribution and species composition of benthic communities may occur as a consequence of changes in climatic conditions (e.g. Harley et al., 2006; Macdonald et al., 2005; Walther et al., 2002). Organisms have three potential ways to respond to changes occurring within a changing environment: (a) they can tolerate changes due to their ecological flexibility, (b) develop adaptations to the new conditions or (c) migrate to areas where the conditions are more suitable (Peck, 2005). Future studies using SDMs and observations will show which way can be applied by specific species.

For grid boxes with sufficient data coverage time series analyses have been carried out. The presented results show that the seasonal signal dominates the variability of temperature for shallow depths on the continental shelf regions. For salinity, the seasonal signal is of less importance. Long term trends are obtained from the de-seasoned time series for both parameters, which are the strongest in shallow depth levels. The majority of the trends is positive, negative trends are only present at deep levels and north of Iceland. This is in agreement with the recently published study of Seidov et al. (2015), who reported a warming of upper ocean

waters in the Nordic Seas and cooling in the deep ocean at depths >500 m. The authors connected the cooling at deeper levels north of Iceland to possible increased cold water inflow from the East Greenland Current. Our negative trends found east of Iceland and in the Faroe Shetland Channel correspond to the cooling area defined in Seidov et al. (2015). The magnitude of trends derived in our study agrees well with the results of Larsen et al. (2012), who estimated similar trends for the core of the Atlantic layer around the Faroe Islands. Warming of the Atlantic inflow into the Nordic Seas was additionally reported in Yashayaev and Seidov (2015), who determined a positive trend of about +0.3 °C/10 years for the shallow coastal waters off Norway for the period 1980–2008 (their Fig. 11, annual data resolution, section NS–S in red). Considering that their estimate is an average of the upper 10–50 m layer and obtained from a section covering a large area, the agreement to our near-bottom temperature trends in the shallow shelf areas is impressive. Salinity trends in Yashayaev and Seidov (2015) are less pronounced and masked by strong interannual variability, which is also similar to the results presented here. Our results indicate that the Atlantic Inflow into the Nordic Seas is getting less dense, while the overflow waters stay the same or even increase in density. Following the results of Eldevik and Nilsen (2013) these increasing thermohaline contrasts lead to a more robust Nordic overturning circulation.

After subtracting the seasonal cycle and the trend from the time series, a substantial residual variability is still evident. No significant connection of the near-bottom residual variability and large scale patters such as the NAO or the AMO is found. Nevertheless, local variability, air–sea–land exchanges and interannual variability additionally impact the analysed hydrographic properties and contribute to the residual variability. In addition, the dynamics of the Subpolar Gyre circulation and the relative contributions of subpolar and subtropical waters to the North Atlantic Current, as described in Hátún et al. (2005), add variability on interannual time scales and are not considered here.
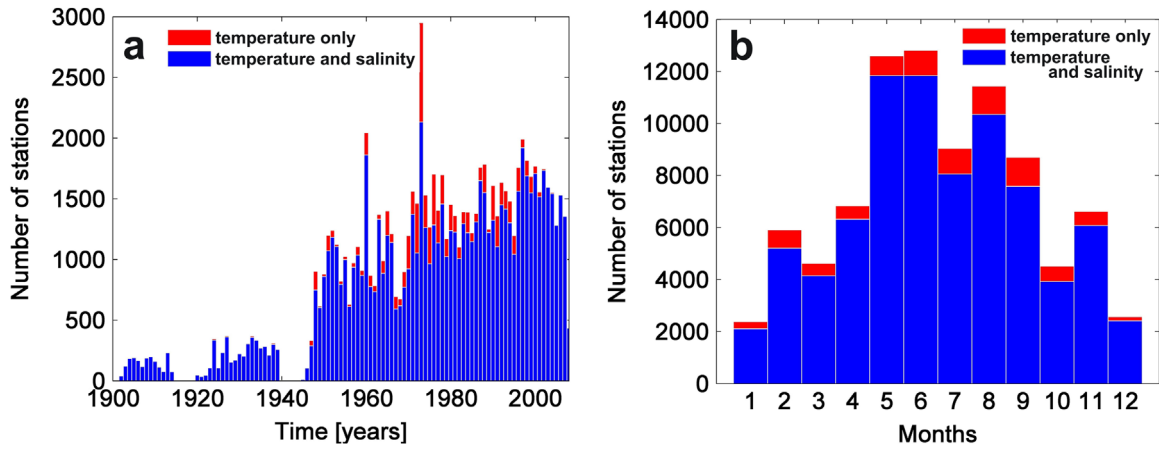
Appendix A

See Figs. A1–A5.

Fig. A1. (a) Number of annual stations used from 1900 to 2008; (b) monthly distribution of the measurements. Blue: number of profiles with both temperature and salinity data; red: number of profiles with temperature data only. In total 88,046 near-bottom temperature and 79,856 near-bottom salinity measurements were used for the analysis after quality control. (For interpretation of the references to color in this figure caption, the reader is referred to the web version of this paper.)
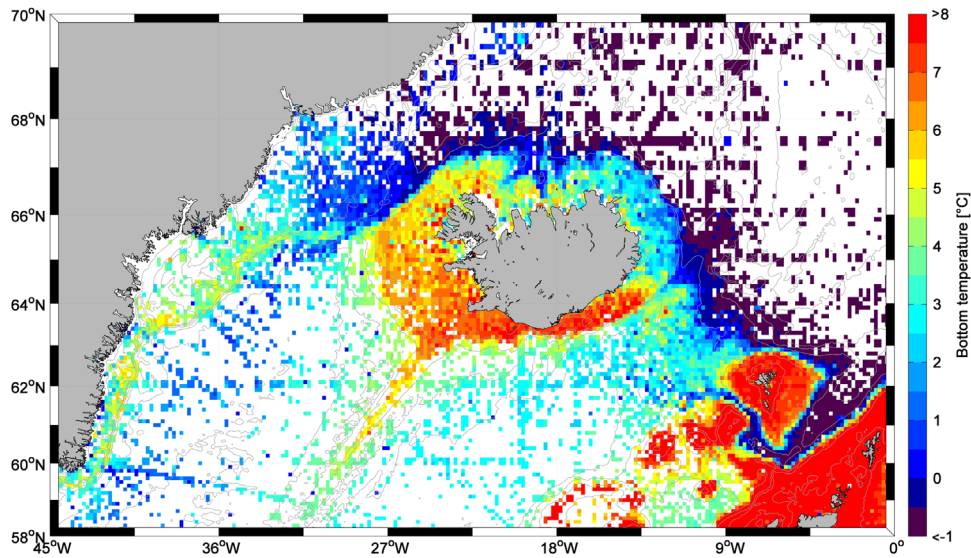

Fig. A2. Gridded average near bottom temperature in the area of investigation using the average of the period 1900–2008. The colorscale has been adjusted to represent the range of most common values; out-of-scale values are included in the red and blue colors of the scale endings. The grid is build by regular steps in longitudinal direction of 0.2° and 0.1° in latitudinal direction. (For interpretation of the references to color in this figure caption, the reader is referred to the web version of this paper.)

Fig. A3. Gridded average near bottom salinity in the area of investigation using the average of the period 1900–2008. The colorscale has been adjusted to represent the range of most common values; out-of-scale values are included in the red and blue colors of the scale endings. The grid is build by regular steps in longitudinal direction of 0.2° and 0.1° in latitudinal direction. (For interpretation of the references to color in this figure caption, the reader is referred to the web version of this paper.)
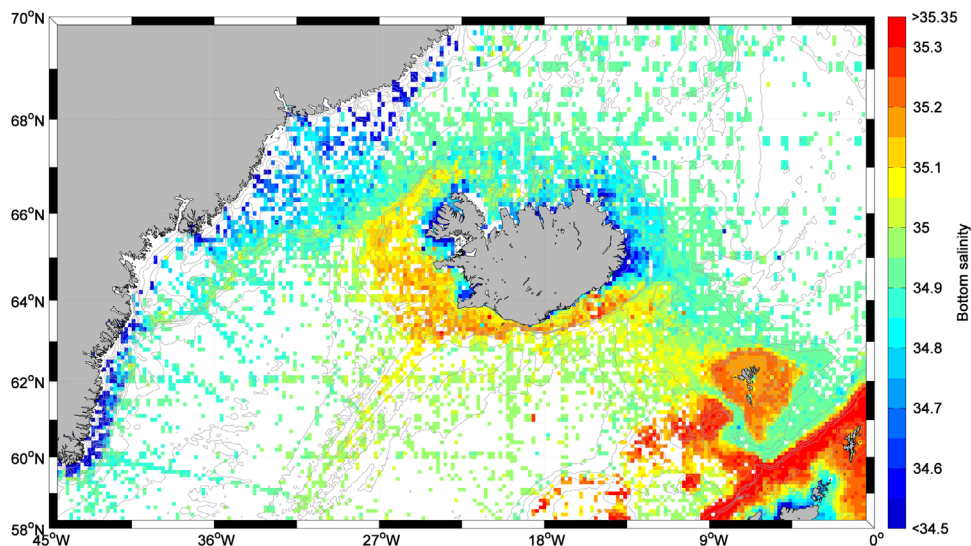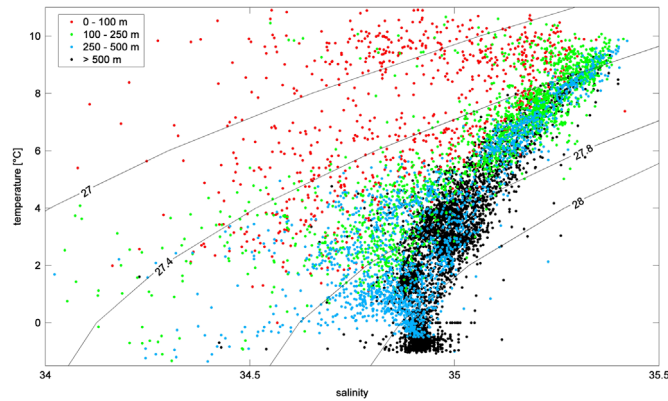
Fig. A4. Temperature–salinity diagram of the gridded data shown in Figs. A2 and A3 with selected isopycnals in black. (For interpretation of the references to color in this figure caption, the reader is referred to the web version of this paper.)
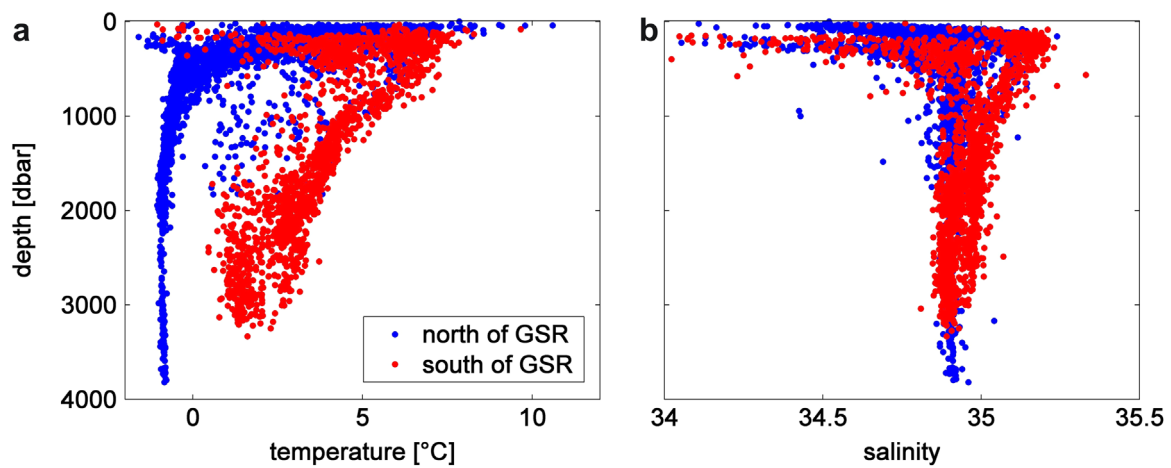

Fig. A5. Temperature profiles (a) and salinity profiles (b) of the gridded data shown in Figs. A2 and A3. Red points denote data from the Irminger Basin (south of 65°N and west of 23°W), while blue points show data from the Iceland and Norwegian Sea (north of 65°N). (For interpretation of the references to color in this figure caption, the reader is referred to the web version of this paper.)

References

Astthorsson, O., Gislason, A., Jonsson, S., 2007. Climate variability and the Icelandic marine ecosystem. Deep-Sea Res. II 54. http://dx.doi.org/10.1016/j.dsr2.2007.07.030.

Brix, S., Svavarsson, J., 2010. Distribution and diversity of desmosomatid and nanoniscid isopods (Crustacea) on the Greenland–Iceland–Faeroe Ridge. Polar Biol. 33. http://dx.doi.org/10.1007/s00300-009-0729-8.

Dauvin, J., Alizier, S., Weppe, A., Gudmundsson, G., 2012. Diversity and zoogeography of Icelandic deep-sea Ampeliscidae (Crustacea: Amphipoda). Deep-Sea Res. I 68. http://dx.doi.org/10.1016/j.dsr.2012.04.013.

Davis, R., 1998. Preliminary results from directly measuring mid-depth circulation in the tropical and South Pacific. J. Geophys. Res. 103. http://dx.doi.org/10.1029/98jc01913.

Dijkstra, H., Warén, A., Gudmundsson, G., 2009. Pectinoidea (Mollusca: Bivalvia) from Iceland. Mar. Biol. Res. 5, 207–243.

Eldevik, T., Nilsen, J., 2013. The arctic–atlantic thermohaline circulation. J. Clim. 26. http://dx.doi.org/10.1175/JCLI-D-13-00305.1.

Elith, J., Graham, C., 2009. Do they? How do they? WHY do they differ? On finding reasons for differing performances of species distribution models. Ecography 32. http://dx.doi.org/10.1111/j.1600-0587.2008.05505.x.

Enfield, D., Mestas-Nunez, A., Trimble, P., 2001. The Atlantic multidecadal oscillation and its relationship to rainfall and river flows in the continental U.S. Geophys. Res. Lett. 28. http://dx.doi.org/10.1029/2000GL012745.

Fer, I., Voet, G., Seim, K., Rudels, B., Latarius, K., 2010. Intense mixing of the Faroe Bank Channel overflow. Geophys. Res. Lett. 37. http://dx.doi.org/10.1029/2009GL041924.

Hansen, B., Østerhus, S., 2000. North Atlantic—Nordic Seas exchanges. Prog. Oceanogr. 45, 109–208.

Harley, C., Hughes, A., Hultgren, K., Miner, B., Sorte, C., Thornber, C., Rodriguez, L., Tomanek, L., Williams, S., 2006. The impacts of climate change in coastal marine systems. Ecol. Lett. 9, 228–241.

Hátún, H., Sandø, A., Drange, H., Hansen, B., Valdimarsson, H., 2005. Influence of the Atlantic Subpolar Gyre on the Thermohaline Circulation. Science 309. http://dx.doi.org/10.1126/science.1116723.

Hurrell, J., 1995. Decadal trends in the North Atlantic oscillation: regional temperatures and precipitation. Science 269, 676–679.

Jakobsson, M., Cherkis, N., Woodward, J., Macnab, R., Coakley, B., 2000. New grid of Arctic bathymetry aids scientists and mapmakers. Eos Trans. 81. http://dx.doi.org/10.1029/00eo00059.

Jónsson, S., Valdimarsson, H., 2005. The flow of Atlantic water into the North Icelandic Shelf and its relation to the drift of cod larvae. ICES J. Mar. Sci. 62, 1350–1359.

Korablev, A., Smirnov, A., Baranova, O., Seidov, D., Parsons, A., 2014. Climatological Atlas of the Nordic Seas and Northern North Atlantic (NODC Accession 0118478). Technical Report NOAA, Washington, DC.

Larsen, K., Hátún, H., Hansen, B., Kristiansen, R., 2012. Atlantic water in the Faroe area: sources and variability. ICES J. Mar. Sci. 69. http://dx.doi.org/10.1093/icesjms/fss028.

Macdonald, R., Harner, T., Fyfe, J., 2005. Recent climate change in the Arctic and its impact on contaminant pathways and interpretation of temporal trend data. Sci. Total Environ. 342, 5–86.

Macrander, A., Käse, R.H., Send, U., Valdimarsson, H., Jónsson, S., 2007. Spatial and temporal structure of the Denmark Strait Overflow revealed by acoustic observations. Ocean Dyn. 57. http://dx.doi.org/10.1007/s10236-007-0101-x.

Mayer, M., Piepenburg, D., 1996. Epibenthic community patterns on the continental slope off East Greenland at 75°N. Mar. Ecol. Prog. Ser. 143. http://dx.doi.org/10.3354/meps143151.

Meißner, K., Fiorentino, D., Schnurr, S., Martinez Arbizu, P., Huettmann, F., Holst, S., Brix, S., Svavarsson, J., 2014. Distribution of benthic marine invertebrates at northern latitudes—an evaluation applying multi-algorithm species distribution models. J. Sea Res. 85. http://dx.doi.org/10.1016/j.seares.2013.05.007.

Nilsen, J., Hatun, H., Mork, K., Valdimarsson, H., 2008. The NISE Dataset. Technical

Report Faroese Fisheries Laboratory, Box 3051, Tórshavn, Faroe Islands.

Østerhus, S., Sherwin, T., Quadfasel, D., Hansen, B., 2008. Arctic–subarctic ocean fluxes. In: Dickson, Meincke, Rhines, S. (Eds.), The Overflow Transport East of Iceland. Arctic–Subarctic Ocean Fluxes. Springer, Netherlands, pp. 427–441.

Østerhus, S., Turrell, W., Jónsson, S., Hansen, B., 2005. Measured volume, heat and salt fluxes from the Atlantic to the Arctic Mediterranean. Geophys. Res. Lett. 32. http://dx.doi.org/10.1029/20054GL022188.

Peck, L., 2005. Prospects for survival in the Southern Ocean: vulnerability of benthic species to temperature change. Antarct. Sci. 17. http://dx.doi.org/10.1017/S0954102005002920.

Schnurr, S., Brandt, A., Brix, S., Fiorentino, D., Malyutina, M., Svavarsson, J., 2014. Composition and distribution of selected munnopsid genera (Crustacea, Isopoda, Asellota) in Icelandic waters. Deep-Sea Res. I 84. http://dx.doi.org/10.1016/j.dsr.2013.11.004.

Seidov, D., Antonov, J., Arzayus, K., Baranova, O., Biddle, M., Boyer, T., Johnson, D., Mishonov, A., Paver, C., Zweng, M., 2015. Oceanography north of 60°N from World Ocean Database. Prog. Oceanogr. 132. http://dx.doi.org/10.1016/j.pocean.2014.02.003.

Sherwin, T., Griffiths, C., Inall, M., Turrell, W., 2008. Quantifying the overflow across the Wyville Thomson Ridge into the Rockall Trough. Deep-Sea Res. I 55, 396–404.

Smith, W., Sandwell, D., 1997. Global sea floor topography from satellite altimetry and ship depth soundings. Science 277, 1956–1962.

Stransky, B., Svavarsson, J., 2010. Diversity and species composition of peracarids (Crustacea: Malacostraca) on the South Greenland shelf: spatial and temporal variation. Polar Biol. 33. http://dx.doi.org/10.1007/s00300-009-0691-5.

Våge, K., Pickart, R., Spall, M., Moore, G., Valdimarsson, H., Torres, D., Erofeeva, S., Nilsen, J., 2013. Revised circulation scheme north of the Denmark Strait. Deep-Sea Res. I 79. http://dx.doi.org/10.1016/j.dsr.2013.05.007.

Voet, G., Quadfasel, D., 2010. Entrainment in the Denmark Strait overflow plume by meso-scale eddies. Ocean Sci. Discuss. 6, 301–310.

Walther, G., Post, E., Convey, P., Menzel, A., Parmesan, C., Beebee, T., Fromentin, J., Hoegh-Guldberg, O., Bairlein, F., 2002. Ecological responses to recent climate change. Nature 416. http://dx.doi.org/10.1038/416389a.

Weisshappel, J., 2001. Distribution and diversity of the hyperbenthic amphipod family Calliopiidae in the different seas around the Greenland–Iceland–Faeroe-Ridge. Sarsia 86, 143–151.

Yashayaev, I., Seidov, D., 2015. The role of the Atlantic Water in multidecadal ocean variability in the Nordic and Barents Seas. Prog. Oceanogr. 132. http://dx.doi.org/10.1016/j.pocean.2014.11.009.